J|A|C|S
ARTICLES
Published on Web 07/25/2006

Supramolecular Self-Assembly of Dendronized Polymers: Reversible Control of the Polymer Architectures through Acid−Base Reactions

Ken C.-F. Leung,[†] Paula M. Mendes,[†] Sergei N. Magonov,[‡] Brian H. Northrop,[†] Sangcheol Kim,[§] Kaushik Patel,[†] Amar H. Flood,[†] Hsian-Rong Tseng,[†] and J. Fraser Stoddart*[,†]

Contribution from the California NanoSystems Institute and Department of Chemistry and Biochemistry, University of California, Los Angeles, 405 Hilgard Avenue, Los Angeles, California 90095-1569, Digital Instruments, Veeco Metrology Group, 112 Robin Hill Road, Santa Barbara, California 93117, and Department of Chemical Engineering, University of California, Santa Barbara, Santa Barbara, California 93106-5080

Received December 1, 2005; E-mail: stoddart@chem.ucla.edu

Abstract: Acid−base switchable supramolecular dendronized polyacetylenes (DPAs) with increasing steric bulk on going from generation one [G1] to three [G3], were constructed using multiple self-assembly processes between Fréchet-type [G1]−[G3]-dendritic dialkylammonium salts and a dibenzo[24]crown-8-containing polymer. The formation of the supramolecular systems is acid−base switchable to either an ON (rodlike dendronized polymers) or an OFF (flexible polymers) state. Thus, by controlling the superstructures of the supramolecular polymers with the [G1]−[G3] dendrons, it is possible to induce conformational changes within the polymer backbones. The supramolecular dendronized polymers, as well as their threading−dethreading properties, were characterized by ^{1}H NMR and UV absorption spectroscopies, gel permeation chromatography (GPC) and light scattering (LS). Independent measures of molecular weight (GPC, LS) indicate that DPAs behave as increasingly rigid macromolecules with each generation in solution. Molecular dynamics simulations of each DPA suggest that the lengths of the polymer backbones increase accordingly. Atomic force microscopy of the [G3]-dendronized polystyrene (DPS), as well as the DPAs, reveal surface morphologies indicative of aggregated superstructures.

Introduction

Recently, the chemical as well as the physical properties of dendritic macromolecules have attracted increasing attention on account of their potential applications as electronic materials.[1] Dendrimers[2] are highly branched, three-dimensional macromolecules comprising several dendritic wedges (dendrons) and a central core. Ideally, they adopt a near-spherical nanoarchitecture at high generations as their steric bulk increases. Alternatively, dendronized polymers[3,4] are based on linear polymers with pendant dendrons as their side chains. One fascinating property of dendronized polymers is that, when several dendrons with higher generations are attached to a linear polymer, they are capable of forcing the random-coiled polymer to afford rigid, rodlike nanocylinders. Percec et al.[5] has recently reported that, in a similar manner, the shape of a polymer can be controlled by the covalent attachment of different dendritic side groups bearing extended alkyl chains. In addition, supramolecular self-assembly using molecular recognition processes, such as hydrogen bonding and metal−ligand interaction, has become a versatile tool for dendrimer construction.[6] Recently, the incorporation of long alkyl chains[7] or other small functional moieties[8] along polymer backbones has also been shown to impose structural control as well as controllable functionalities.

The self-assembling functionalization on polymers usually requires high-affinity binding recognition motifs between small molecular components and polymers. One example of such high-

[†] University of California, Los Angeles.
[‡] Digital Instruments, Veeco Metrology Group.
[§] University of California, Santa Barbara.

(1) Percec, V.; et al. *Nature* **2002**, *419*, 384−387.
(2) For reviews, see: (a) Fréchet, J. M. J.; Tomalia, D. A. *Dendrimers and Other Dendritic Polymers*, Wiley: New York, 2002. (b) Newkome, G. R.; Vögtle, F.; Moorefield, C. N. *Dendrimers and Dendrons: Concepts, Syntheses, Applications*; VCH: New York, 2001. (c) Chow, H.-F.; Mong, T. K.-K.; Nongrum, M. F.; Wan, C.-W. *Tetrahedron* **1998**, *54*, 8543−8660. (d) Matthews, O. A.; Shipway, A. N.; Stoddart, J. F. *Prog. Polym. Sci.* **1998**, *23*, 1−56. (e) Bosman, A. W.; Janssen, H. M.; Meijer, E. W. *Chem. Rev.* **1999**, *99*, 1665−1688. (f) Stoddart, F. J.; Welton, T. *Polyhedron* **1999**, *18*, 3575−3591. (g) Vögtle, F.; Gestermann, S.; Hesse, R.; Schwierz, H.; Windisch, B. *Prog. Polym. Sci.* **2000**, *25*, 987−1041.
(3) For reviews, see: (a) Frey, H. *Angew. Chem., Int. Ed.* **1998**, *37*, 2193-2197. (b) Schlüter, A. D.; Rabe, J. P. *Angew. Chem., Int. Ed.* **2000**, *39*, 864−883. (c) Schlüter, A. D. *Top. Curr. Chem.* **2005**, *245*, 151−191. (d) Frauenrath, H. *Prog. Polym. Sci.* **2005**, *30*, 325−384.
(4) For selected examples, see: (a) Zhang, A.; Okrasa, L.; Pakula, T.; Schlüter, A. D. *J. Am. Chem. Soc.* **2004**, *126*, 6658−6666. (b) Helms, B.; Mynar, J. L.; Hawker, C. J.; Fréchet, J. M. J. *J. Am. Chem. Soc.* **2004**, *126*, 15020−15021. (c) Li, W.-S.; Jiang, D.-L.; Aida, T. *Angew. Chem., Int. Ed.* **2004**, *43*, 2943−2947. (d) Yoshida, M.; Fresco, Z. M.; Ohnishi, S.; Fréchet, J. M. J. *Macromolecules* **2005**, *38*, 334−344. (e) Percec, V.; et al. *J. Am. Chem. Soc.* **2005**, *127*, 15257-15264. (f) Shenhar, R.; Xu, H.; Frankamp, B. L.; Mates, T. E.; Sanyal, A.; Uzun, O.; Rotello, V. M. *J. Am. Chem. Soc.* **2005**, *127*, 16318−16324.
(5) (a) Percec, V.; Ahn, C.-H.; Ungar, G.; Yeardley, D. J. P.; Möller, M.; Sheiko, S. S. *Nature* **1998**, *391*, 161−164. (b) Percec, V.; et al. *Nature* **2004**, *430*, 764−768.

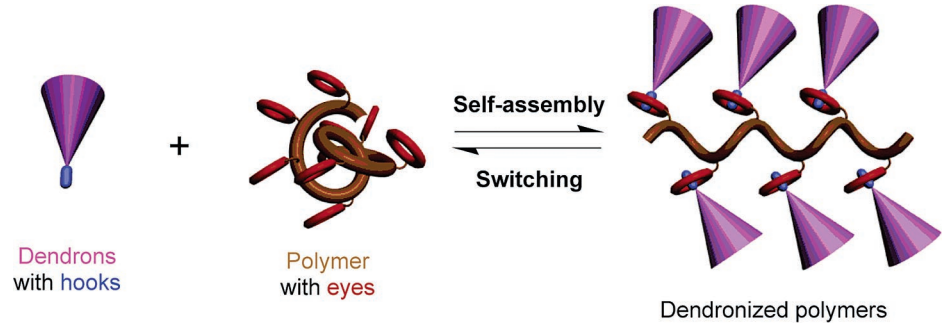

Figure 1. Schematic representation of the supramolecular self-assembly of dendronized polymers constructed using multiple self-assembly between dendritic dialkylammonium salts (hooks) and the crown ether (eyes) containing polymer, in a process which induces conformational changes upon the polymer backbone. The formation of the supramolecular systems are acid−base switchable between an ON (rigid dendronized polymers) and an OFF (flexible polymers) state.

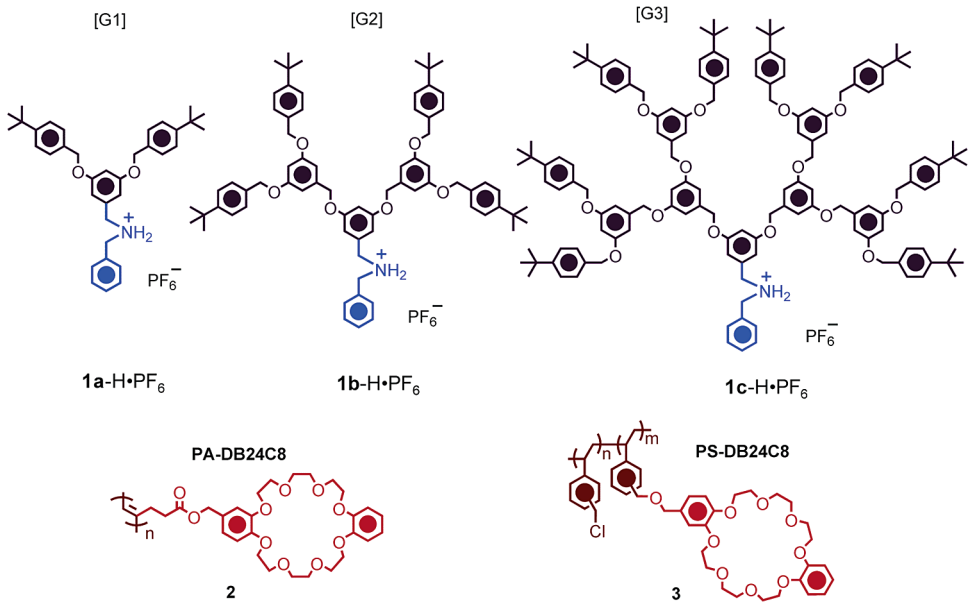

Figure 2. Structural formulas of the [G1]−[G3]-dendritic dialkylammonium salts **1a**−**c**-H•PF_6, the polyacetylene PA-DB24C8 (**2**) and the polystyrene PS-DB24C8 (**3**).

affinity binding recognition motifs is the complexation[9,10] between dialkylammonium ion centers ($-CH_2NH_2^+CH_2-$) and a crown ether unit, e.g. dibenzo[24]crown-8 (DB24C8). By mixing such components together in 1:1 molar ratio, it results in the formation of a pseudorotaxane complex held by strong [$N^+-H\cdots O$] hydrogen bonds between the acidic NH_2^+ protons and the oxygen atoms in the DB24C8 ring. Moreover, additional [$C-H\cdots O$] and $\pi-\pi$ stacking interactions, as well as electrostatic forces, also contribute to the stability of the pseudorotaxane's formation. Specifically, by taking advantage of the complexation known to occur between the $-CH_2NH_2^+CH_2-$ (hooks) and the DB24C8 (eyes), as well as its acid−base switching properties in solution,[11] we report herein a class of acid−base switchable supramolecular dendronized polymers (Figure 1) based on a conducting polymer[12]−polyacetylene and a nonconducting polymer−polystyrene as backbones. First, the generation one [G1] to generation three [G3]-dendronized

(6) For selected examples, see: (a) Zimmerman, S. C.; Zeng, F.; Reichert, D. E. C.; Kolotuchin, S. V. *Science* **1996**, *271*, 1095−1098. (b) Amabilino, D. B.; et al. *J. Am. Chem. Soc.* **1996**, *118*, 12012-12020. (c) Yamaguchi, N.; Hamilton, L. M.; Gibson, H. W. *Angew. Chem., Int. Ed.* **1998**, *37*, 3275−3279. (d) Hübner, G. M.; Nachtsheim, G.; Li, Q. Y.; Seel, C.; Vögtle, F. *Angew. Chem., Int. Ed.* **2000**, *39*, 1269−1272. (e) Yamaguchi, N.; Gibson, H. W. *Macromol. Chem. Phys.* **2000**, *201*, 815−824. (f) Osswald, F.; Vogel, E.; Safarowsky, O.; Schwanke, F.; Vögtle, F. *Adv. Synth. Catal.* **2001**, *343*, 303−309. (g) Gibson, H. W.; Yamaguchi, N.; Hamilton, L. M.; Jones, J. W. *J. Am. Chem. Soc.* **2002**, *124*, 4653−4665. (h) Jones, J. W.; Bryant, W. S.; Bosman, A. W.; Janssen, R. A. J.; Meijer, E. W.; Gibson, H. W. *J. Org. Chem.* **2003**, *68*, 2385−2389. (i) Leung, K. C.-F.; Aricó, F.; Cantrill, S. J.; Stoddart, J. F. *J. Am. Chem. Soc.* **2005**, *127*, 5808−5810. (j) Zong, Q.-S.; Zhang, C.; Chen, C.-F. *Org. Lett.* **2006**, *8*, 1859−1862.

(7) (a) Ruokolainen, J.; Mäkinen, R.; Torkkeli, M.; Mäkelä, T.; Serimaa, R.; ten Brinke, G.; Ikkala, O. *Science* **1998**, *280*, 557−560. (b) Mäki-Ontto, R.; de Moel, K.; de Odorico, W.; Ruokolainen, J.; Stamm, M.; ten Brinke, G.; Ikkala, O. *Adv. Mater.* **2001**, *13*, 117−121. (c) Ikkala, O.; ten Brinke, G. *Science* **2002**, *295*, 2407−2409.

(8) (a) Oku, T.; Furusho, Y.; Takata, T. *Angew. Chem., Int. Ed.* **2004**, *43*, 966−969. (b) Pollino, J. M.; Weck, M. *Chem. Soc. Rev.* **2005**, *34*, 193−207 and references therein; (c) South, C. R.; Higley, M. N.; Leung, K. C.-F.; Lanari, D.; Nelson, A.; Grubbs, R. H.; Stoddart, J. F.; Weck, M. *Chem. Eur. J.* **2006**, 3789−3797. (d) South, C. R.; Leung, K. C.-F.; Lanari, D.; Stoddart, J. F.; Weck, M. *Macromolecules* **2006**, *39*, 3738−3744.

(9) Kolchinski, A. G.; Busch, D. H.; Alcock, N. W. *J. Chem. Soc., Chem. Commun.* **1995**, 1289−1291.

(10) (a) Ashton, P. R.; Campbell, P. J.; Chrystal, E. J. T.; Glink, P. T.; Menzer, S.; Philp, D.; Spencer, N.; Stoddart, J. F.; Tasker, P. A.; Williams, D. J. *Angew. Chem., Int. Ed. Engl.* **1995**, *34*, 1865−1869. (b) Ashton, P. R.; Campbell, P. J.; Chrystal, E. J. T.; Glink, P. T.; Menzer, S.; Schiavo, C.; Stoddart, J. F.; Tasker, P. A.; Williams, D. J. *Angew. Chem., Int. Ed. Engl.* **1995**, *34*, 1869−1871. (c) Ashton, P. R.; et al. *Chem. Eur. J.* **1996**, *2*, 709−728. (d) Glink, P. T.; Schiavo, C.; Stoddart, J. F. *Chem. Commun.* **1996**, 1483−1490. (e) Martínez-Díaz, M. V.; Spencer, N.; Stoddart, J. F. *Angew. Chem., Int. Ed. Engl.* **1997**, *36*, 1904−1907. (f) Rowan, S. J.; Cantrill, S. J.; Stoddart, J. F. *Org. Lett.* **1999**, *1*, 129−132. (g) Cantrill, S. J.; Pease, A. R.; Stoddart, J. F. *J. Chem. Soc., Dalton Trans.* **2000**, 3715−3734. (h) Rowan, S. J.; Stoddart, J. F. *J. Am. Chem. Soc.* **2000**, *122*, 164−165. (i) Chiu, S.-H.; Rowan, S. J.; Cantrill, S. J.; Stoddart, J. F.; White, A. J. P.; Williams, D. J. *Chem. Eur. J.* **2002**, *8*, 5170−5183. (j) Aricó, F.; Badjic, J. D.; Cantrill, S. J.; Flood, A. H.; Leung, K. C.-F.; Liu, Y.; Stoddart, J. F. *Top. Curr. Chem.* **2005**, *249*, 203−259.

Scheme 1 [a]

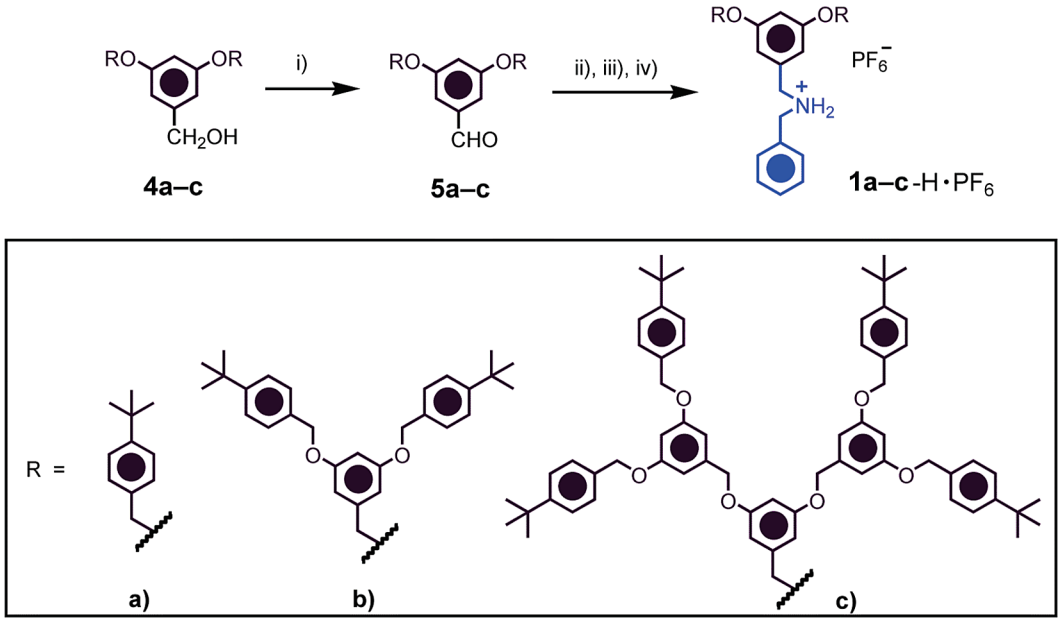

[a] Reagents and conditions: i) PCC, CH_2Cl_2, 25 °C, 2 h; ii) benzylamine, PhMe, 110 °C, 2 h; iii) $NaBH_4$, MeOH, THF, 0−25 °C, 6 h; iv) HPF_6, H_2O, THF, 0 °C, 30 min.

polyacetylenes (DPAs) [**1a**−**c**-H·PF_6]$_n$⊂**2** were constructed by self-assembly of multiple [G1]−[G3]-dendritic dialkylammonium salts **1a**−**c**-H·PF_6 with PA-DB24C8 (**2**) via noncovalent bonding (Figure 2). Furthermore, the dendronized polystyrenes (DPSs) [**1a**−**c**-H·PF_6]$_n$⊂**3** were constructed by the self-assembly of [G1]−[G3]-dendritic dialkylammonium salts **1a**−**c**-H·PF_6 with PS-DB24C8 (**3**). The formation of the dendronized polymers was demonstrated to be controllable by acid−base reactions, which revealed that the system could be switched to rigid dendronized polymers (ON) and to flexible polymers (OFF) reversibly. Rodlike dendronized polymers can be formed by chemically controlling the interpenetration of the dendrons to induce conformational changes of the linear polymer backbone. These investigations have illustrated how synthesis can be utilized, in conjunction with switchable building blocks, to control if and when polymer backbones form either rigid or flexible structures.

Results and Discussion

Synthesis. The [G1]−[G3]-dendritic dialkylammonium salts **1a**−**c**−H·PF_6 were synthesized[13] starting from their corresponding [G1]−[G3]-dendritic alcohols **4a**−**c** (Scheme 1). The syntheses of the precursor [G1]−[G3]-dendritic aldehydes **5a**−**c** were achieved by the oxidation of [G1]−[G3]-dendritic alcohols **4a**−**c** using pyridinium chlorochromate (PCC). Subsequently, the aldehydes **5a**−**c** were treated with benzylamine, the imines that were formed were reduced with sodium borohydride, and protonation of the secondary amines were completed with hydrogen hexafluorophosphate solution. The "short" *cis*−*transoidal* polyacetylene PA-DB24C8 (**2**) was prepared (Scheme 2) starting from the macrocyclic alcohol **6**,[14] with a weight-average molecular weight (M_w) of 18 kDa, a number-average molecular weight (M_n) of 13 kDa, a degree of polymerization (DP) of 33, and a polydispersity index (PDI) of 1.4 as determined by light scattering (LS) techniques in CH_2Cl_2 at 298 K. First, the alcohol **6** was coupled with 4-pentynoic acid using *N*,*N*′-dicyclohexylcarbodiimide (DCC) in the presence of a catalytic amount of 4-(dimethylamino)pyridine (DMAP) to afford the macrocyclic monomer **7**. Then, the monomer **7** was further polymerized to give the polyacetylene PA-DB24C8 (**2**) using $[Rh(nbd)Cl]_2$ (10 mol %, nbd = norbornadiene) as the catalyst. The "long" polystyrene PS-DB24C8 (**3**) (M_w = 140 kDa, M_n = 85 kDa, DP = 650, and PDI = 1.7 determined by LS with ∼50% crown ether attachment, i.e., m = n ∼ 1:1) was synthetically modified from commercially available poly(vinylbenzyl chloride) (M_w = 100 kDa, M_n = 55 kDa and PDI = 1.8) by direct alkylation with the alcohol **6**.

Scheme 2 [a]

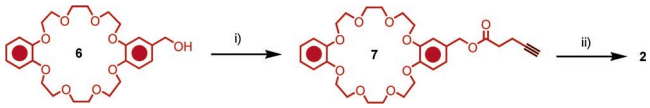

[a] Reagents and conditions: i) 4-Pentynoic acid, DCC, DMAP, CH_2Cl_2, 25 °C, 12 h; ii) $[Rh(nbd)Cl]_2$, Et_3N, CH_2Cl_2, 25 °C, 24 h.

Characterization. The supramolecular self-assembly between equivalent amounts (1:1 crown ether/ammonium ion) of the [G1]−[G3]-dendritic dialkylammonium salts **1a**−**c**-H·PF_6 with polyacetylene PA-DB24C8 (**2**) to form supramolecular [G1]−

(11) (a) Ashton, P. R.; et al. *J. Am. Chem. Soc.* **1998**, *120*, 11932-11942. (b) Balzani, V.; Credi, A.; Raymo, F. M.; Stoddart, J. F. *Angew. Chem., Int. Ed.* **2000**, *39*, 3348−3391. (c) Elizarov, A. M.; Chiu, S.-H.; Stoddart, J. F. *J. Org. Chem.* **2002**, *67*, 9175−9181. (d) Badjic, J. D.; Balzani, V.; Credi, A.; Silvi, S.; Stoddart, J. F. *Science* **2004**, *303*, 1845−1849. (e) Badjic, J. D.; Ronconi, C. M.; Stoddart, J. F.; Balzani, V.; Silvi, S.; Credi, A. *J. Am. Chem. Soc.* **2006**, *128*, 1489−1499.

(12) (a) McQuade, D. T.; Pullen, A. E.; Swager, T. M. *Chem. Rev.* **2000**, *100*, 2537−2574. (b) Shirakawa, H. *Angew. Chem., Int. Ed.* **2001**, *40*, 2574−2580. (c) MacDiarmid, A. G. *Angew. Chem., Int. Ed.* **2001**, *40*, 2581−2590. (d) Heeger, A. J. *Angew. Chem., Int. Ed.* **2001**, *40*, 2591−2611. (e) Nonokawa, R.; Yashima, E. *J. Am. Chem. Soc.* **2003**, *125*, 1278−1283. (f) Nonokawa, R.; Yashima, E. *J. Polym. Sci. A* **2003**, *41*, 1004−1013. (g) Nonokawa, R.; Oobo, M.; Yashima, E. *Macromolecules* **2003**, *36*, 6599−6606. (h) Cheuk, K. K. L.; Lam, J. W. Y.; Chen, J.; Lai, L. M.; Tang, B. Z. *Macromolecules* **2003**, *36*, 5947−5959. (i) Lam, J. W. Y.; Tang, B. Z. *Acc. Chem. Res.* **2005**, *38*, 745−754.

(13) Stoddart, A.; et al. *Helv. Chim. Acta* **2001**, *84*, 296−334.

(14) Diederich, F.; Echegoyen, L.; Gómez-López, M.; Kessinger, R.; Stoddart, J. F. *J. Chem. Soc., Perkin Trans. 2* **1999**, 1577−1586.

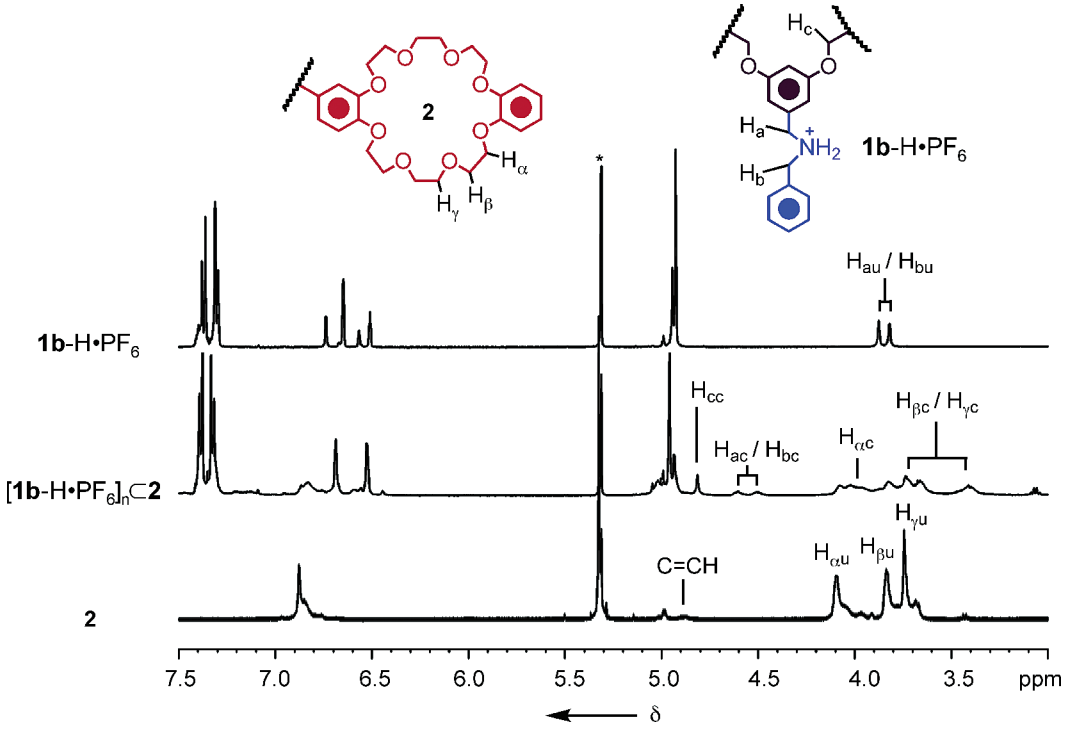

Figure 3. Partial ^{1}H NMR (500 MHz, CD_2Cl_2, 298 K, 20 mM) spectra of the [G2]-dendritic ammonium salt **1b**-H·PF_6, the [G2]-DPA [**1b**-H·PF_6]$_n$⊂**2** and the polyacetylene PA-DB24C8 (**2**) (u = uncomplexed, c = complexed, and * = solvent residue).

[G3]-DPAs [**1a**−**c**-H·PF_6]$_n$⊂**2**, was examined by ^{1}H NMR spectroscopy (CD_2Cl_2, 500 MHz, 298 K). The ^{1}H NMR spectra were obtained after 15 min of mixing between the solutions of [G1]−[G3]-dendritic ammonium salts **1a**−**c**-H·PF_6 and **2** (total concentration = 20 mM). By way of an example, the partial ^{1}H NMR spectrum (Figure 3) of the [G2]-DPA [**1b**-H·PF_6]$_n$⊂**2** reveals that the characteristic benzylic methylene proton signals adjacent to the ammonium ion center observed at 3.8−3.9 ppm in the [G2]-dendritic ammonium salt **1b**-H·PF_6 are shifted downfield to 4.5−4.6 ppm upon complexation. Furthermore, the characteristic peaks for the protons on the crown ether (H_α, H_β, and H_γ), which resonate at 4.10, 3.82 and 3.72 ppm in the PA-DB24C8 (**2**), are shifted upfield to 3.96, 3.70 and 3.42 ppm in the spectrum of the [G2]-DPA [**1b**-H·PF_6]$_n$⊂**2**, respectively. These shifts of the NMR signals indicate that the dialkylammonium ions on the dendron are encircled by the crown ether moieties on the polymer backbone, thus forming dendritic [2]pseudorotaxanes.[10a,b] The percentage attachments of dendrons onto the PA-DB24C8 (**2**), which originated from their NMR signal intensities of the characteristic peak, were calculated to be 92%, 85%, and 70% for the [G1]-, [G2]-, and [G3]-dendrons, respectively, by comparing the ratio of average integrals between the complexed and uncomplexed NMR signals. However, the calculation from the NMR signal intensities has about ±5% error, and the error may be even larger for the case of [G3]-DPA on account of the low signal intensities observed. When similar complexation experiments were carried out using an excess of **1a**−**c**-H·PF_6 to PA-DB24C8 (**2**), the degree of complexation remains almost unchanged from the NMR spectra. Moreover, the ^{1}H NMR spectra of the [G1]−[G3]-DPAs [**1a**−**c**-H·PF_6]$_n$⊂**2** do not show any significant change after prolonged standing, at least for 24 h, an observation which reveals that the superstructures are stable in CH_2Cl_2 solution.

Table 1. Gel Permeation Chromatography and Light-Scattering Results

	GPC[a]			LS[b]			
structure	M_w/ kDa	M_n/ kDa	PDI	M_w/ kDa	M_n/ kDa	PDI	R_h/ nm
2	15	9.3	1.6	18	13	1.4	93
[**1a**-H·PF_6]$_n$⊂**2**	19	11	1.7	38	25	1.5	98
[**1b**-H·PF_6]$_n$⊂**2**	24	13	1.8	52	30	1.7	105
[**1c**-H·PF_6]$_n$⊂**2**	29	15	1.9	70	36	1.9	112

[a] CH_2Cl_2, 298 K, polystyrene standards. [b] CH_2Cl_2, 293 K.

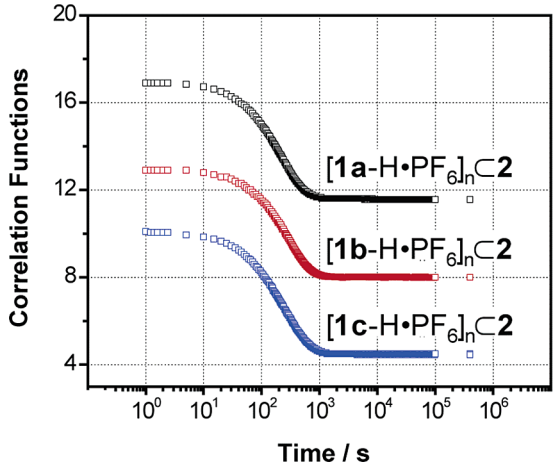

Figure 4. Plot of correlation functions versus time for the measurement of hydrodynamic radii (R_h) of [G1]−[G3]-DPAs [**1a**−**c**-H·PF_6]$_n$⊂**2** by dynamic light scattering.

The relative and absolute molecular weights of [G1]−[G3]-DPAs [**1a**−**c**-H·PF_6]$_n$⊂**2** were determined using gel permeation chromatography (GPC) and dynamic LS, respectively. Static LS is not employed in this study because the supramolecular complexation between the dendritic ammonium salts and the

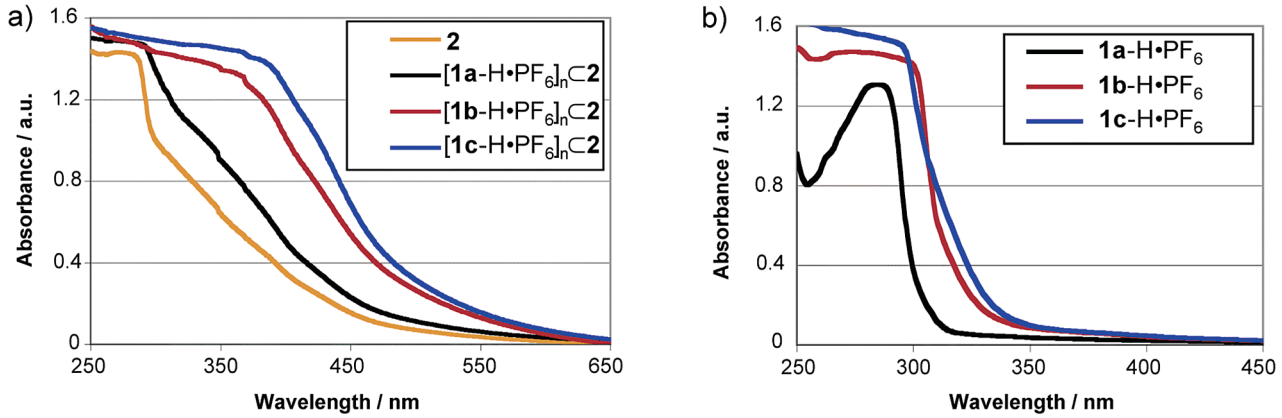

Figure 5. UV/visible absorption spectra of (a) the polyacetylene PA-DB24C8 (**2**) and the [G1]−[G3]-DPAs [**1a**−**c**-H•PF_6]$_n$⊂**2** (0.33 mg/mL, CH_2Cl_2, 298 K) and (b) the [G1]−[G3]-dendritic ammonium salts **1a**−**c**-H•PF_6 (0.33 mg/mL, CH_2Cl_2, 298 K).

crown ether-containing polymers is concentration dependent, such that the determination of the refractive index of increment (*dn*/*dc*) of the superstructure is somewhat difficult to achieve. The M_n values (Table 1) determined by GPC and LS varies slightly (GPC: from 9.3 kDa to 15 kDa; LS: from 13 kDa to 36 kDa) of **2** and [**1a**−**c**-H•PF_6]$_n$⊂**2**. Importantly, these results revealed that approximately similar numbers of the [G1]- to [G3]-dendritic ammonium salts are complexed with each polymer chain. Moreover, the hydrodynamic radii (R_h) (Figure 4) determined by LS increases from 93 nm for **2**, to 98, 105, and 112 nm for [**1a**−**c**-H•PF_6]$_n$⊂**2**, respectively, which indicates that the size of the polymer increases after the attachment of dendrons.

Table 2. Comparison of the Percentage of Dendron Attachment onto the Polymer Backbone Calculated from LS and NMR Spectroscopy as Well as the Ratio of the Molecular Weights Determined by LS and GPC

structure	% dendron attachment		M_w (LS)/ M_w (GPC)	M_n (LS)/ M_n (GPC)
	LS	NMR		
2	–	–	1.2	1.4
[**1a**-H•PF_6]$_n$⊂**2**	91	92	2.0	2.3
[**1b**-H•PF_6]$_n$⊂**2**	86	85	2.2	2.3
[**1c**-H•PF_6]$_n$⊂**2**	70	70	2.4	2.4

The M_w determined by using LS reveals the percentage attachment of dendrons to the PA-DB24C8 (**2**): they are calculated to be 91%, 86%, and 70% for [G1]-, [G2]-, and [G3]-dendrons, respectively (Table 2). Comparatively, the percentages of dendron attachment, determined from the average integrals of the characteristic NMR signal, are calculated to be 92%, 85%, and 70% with [G1]-, [G2]-, and [G3]-dendrons, respectively, which are consistent with the calculated values obtained from LS. The molecular weight values determined using both GPC and LS of polymer **2** are similar. The ratios of M_w(LS)/M_w(GPC), parameters which indicate the magnitudes of the deviations from polystyrene standards,[3b,15] increase significantly with rising generations of the dendrons. This ratio reflects that the rigidity of the system is increasing by the attachment of dendrons with increasing bulk. Moreover, the ratios of M_n(LS)/M_n(GPC) are similar for the [G1]- to [G3]-DPAs [**1a**−c-H•PF_6]$_n$⊂**2**, which demonstrated that both the GPC and the LS analyses revealed similar magnitude of increments with their M_n value.

(15) Chow, H.-F.; Leung, C.-F.; Li, W.; Wong, K.-W.; Xi, L. *Angew. Chem., Int. Ed.* **2003**, *42*, 4919−4923.

The UV/visible absorption spectra of PA-DB24C8 (**2**) (0.33 mg/mL, CH_2Cl_2, 298 K) show (Figure 5a) a typical long-range band arising from internal electronic transitions: the continuous absorption, which ends at about 550 nm, is a common UV absorption profile for functionalized polyacetylenes.[12h] However, the UV/visible spectra of the [G1]−[G3]-DPAs [**1a**−**c**-H•PF_6]$_n$⊂**2** (0.33 mg/mL, fixed concentration of PA-DB24C8) show a red-shift in the UV absorption region with rising generations of dendrons as a result of conformational changes in the PA-DB24C8 (**2**) backbones, induced by the formation of supermolecules. The observation of the red-shift indicates the extension of the conjugation length of the polyacetylene backbone. In contrast, the UV/visible absorption spectra (Figure 5b) of [G1]−[G3]-dendritic dialkylammonium salts (0.33 mg/mL, CH_2Cl_2, 298 K) reveal maximum absorptions ranging from 280 to 300 nm.

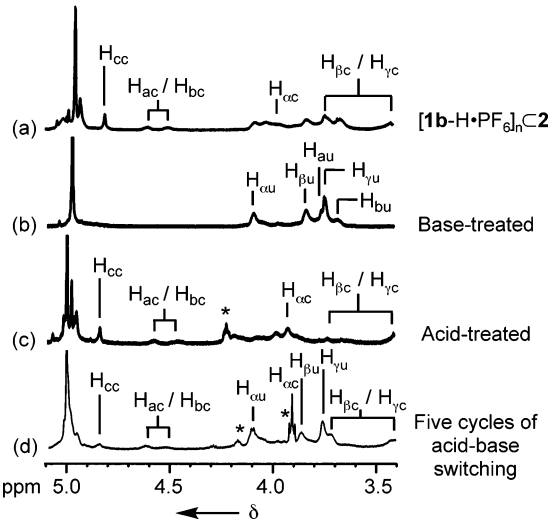

Figure 6. Partial ^{1}H NMR (500 MHz, CD_2Cl_2, 20 mM) spectra of (a) [G2]-DPA [**1b**-H•PF_6]$_n$⊂**2**, (b) base-treated, (c) acid-treated, and (d) acid−base switching after five cycles of the [G2]-DPA [**1b**-H•PF_6]$_n$⊂**2** (u = uncomplexed, c = complexed, and * = impurities).

The acid−base switching properties of the supramolecular polymer [G1]−[G3]-DPAs [**1a**−**c**-H•PF_6]$_n$⊂**2** were monitored by ^{1}H NMR spectroscopy (20 mM, CD_2Cl_2, 298 K). As an example, upon treatment of the [G2]-DPA [**1b**-H•PF_6]$_n$⊂**2** with 1.1 equiv (per crown ether) of the base (Et_3N), the ^{1}H NMR spectrum indicates that the characteristic signals (Figure 6a) at 4.5−4.6 ppm—originating from the benzylic methylene protons

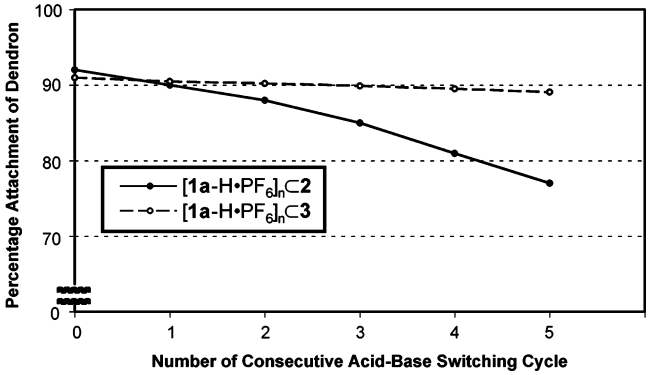

Figure 7. Plot of the percentage attachment versus the number of consecutive acid−base switching of the [G1]-DPA [**1a**-H•PF_6]$_n$⊂**2** (solid circle) and [G1]-DPS [**1a**-H•PF_6]$_n$⊂**3** (open circle).

adjacent to the NH_2^+ ion center—disappear (Figure 6b). These observations suggest that the [G2]-dendrons **1b**-H•PF_6 were deprotonated and subsequently dethreaded from the cavity of each DB24C8 side group on the polymer (**2**) to give the separate products (**1b** and **2**). Upon addition of 1.2 equiv (per crown ether) of trifluoroacetic acid to the same solution, however, the characteristic signals at 4.5−4.6 ppm were installed (Figure 6c), confirming that recomplexation has occurred, leading to the reformation of the conformationally rigid supramolecular polymer [G2]-DPA [**1b**-H•TFA]$_n$⊂**2** (TFA = trifluoroacetate). Figure 6d shows the NMR spectrum of the [G2]-DPA [**1b**-H•PF_6]$_n$⊂**2** after five cycles of the acid−base switching, which also shows the integrities of the supramolecular complexation between the dendritic ammonium salts and the polymer (4.5−4.6 ppm). However, the spectrum (Figure 6d) also reveals that some of the uncomplexed crown ethers ($H_{\alpha u}$, $H_{\beta u}$, and $H_{\gamma u}$ where u = uncomplexed) on the polymer are present, which may account for the degradations of the dendritic ammonium salt and the polyacetylene backbone after several cycles of acid−base switching.

This acid−base switching process could be repeated at least five cycles for all the [G1]- to [G3]-DPAs and DPSs with the observation of the supramolecular complexation from their NMR spectra with minimal degradation, hence illustrating the power of switching to control the rigidity of the polymer backbone by successive additions of acid and base. Figure 7 shows the plot of the percentage attachment of the [G1]-dendron onto the polymer backbone of both the DPA (**2**) and DPS (**3**) from the solutions of [**1a**-H•PF_6]$_n$⊂**2** and [**1a**-H•PF_6]$_n$⊂**3** (20 mM, CD_2Cl_2, 298 K) versus the number of consecutive cycles of the acid−base switching process calculated from their NMR spectra (see Supporting Information). Comparatively, after five cycles of the acid−base switching, [G1]-DPS has 89% of the dendron attachment, whereas [G1]-DPA has only 77%, which demonstrated that the supramolecular DPSs are more robust than that of the DPAs upon acid−base switching. Moreover, the density of DB24C8 on the PS-DB24C8 (**3**) should be low enough such that two adjacent dendrons attached are relatively far away which enhances the formation of the DPS. One drawback of this acid−base switching process is that it generates the salt Et_3NH•TFA or Et_3NH•PF_6, after each cycle of acid−base neutralization. The accumulation of the salts after several switching processes will eventually affect the supramolecular complexation and the characterization of resulting superstructures, e.g., with UV/vis and NMR spectroscopies.

Atomic force microscopic (AFM) studies were performed to obtain information about the morphology of the dendronized polymers upon self-assembly of [G3]-dendrons **1c**-H•PF_6 with either PA-DB24C8 (**2**) or PS-DB24C8 (**3**). Samples were prepared by immersing vertically freshly cleaved highly oriented pyrolytic graphite (HOPG) substrates in CH_2Cl_2 solutions (50 mg/mL) for 20 s. On account of both the softness and short size of the [G3]-DPA [**1c**-H•PF_6]$_n$⊂**2** molecules, their morphology on HOPG surfaces could not be resolved by AFM. However, [G3]-DPS [**1c**-H•PF_6]$_n$⊂**3** were characterized (Figure 8a) as having wormlike structures with diameters of 2−3 nm,[16] in addition to also displaying their aggregated superstructures. This morphology contrasts with that observed (Figure 8b) for PS-DB24C8 (**3**), which shows a network of globular features with a narrow height distribution of about 3 nm. By contrast, the [G3]-dendrons **1c**-H•PF_6 were characterized by forming a monolayer (Figure 8c) with local globular aggregates (~8 nm height).

Simulations. The impact of complexation on the conformations of the DPAs was investigated (Figure 9) using molecular dynamics simulations. The parent PA-DB24C8 (**2**) and [G1]−[G3]-DPAs [**1a**−**c**-H•PF_6]$_n$⊂**2**, all with a degree of polymerization of 40, were equilibrated for 300 ps using the AMBER* force field[17] and the GB/SA solvent model[18] for $CHCl_3$ in the program[19] Maestro v3.0.038. The parent PA-DB24C8 (**2**) is shown to be "linear" with an average length of 9.8 nm and an average diameter of 2.6 nm. Upon complexation, each DPA becomes longer (13.0−14.4 nm) and wider in diameter (4.5−6.0 nm). These simulation results are correlated to the experimental observation in the UV/visible absorption spectra with

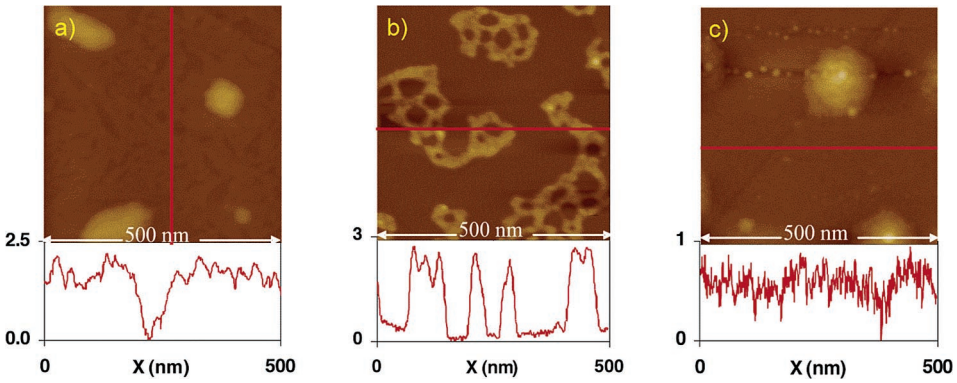

Figure 8. AFM images and their respective cross-sectional profiles of (a) the [G3]-DPS ([**1c**-H•PF_6]$_n$⊂**2**), (b) the PS-DB24C8 (**3**), and (c) the [G3]-dendrons **1c**-H•PF_6 on HOPG substrates prepared by vertical immersion from a 50 mg/mL CH_2Cl_2 solution.

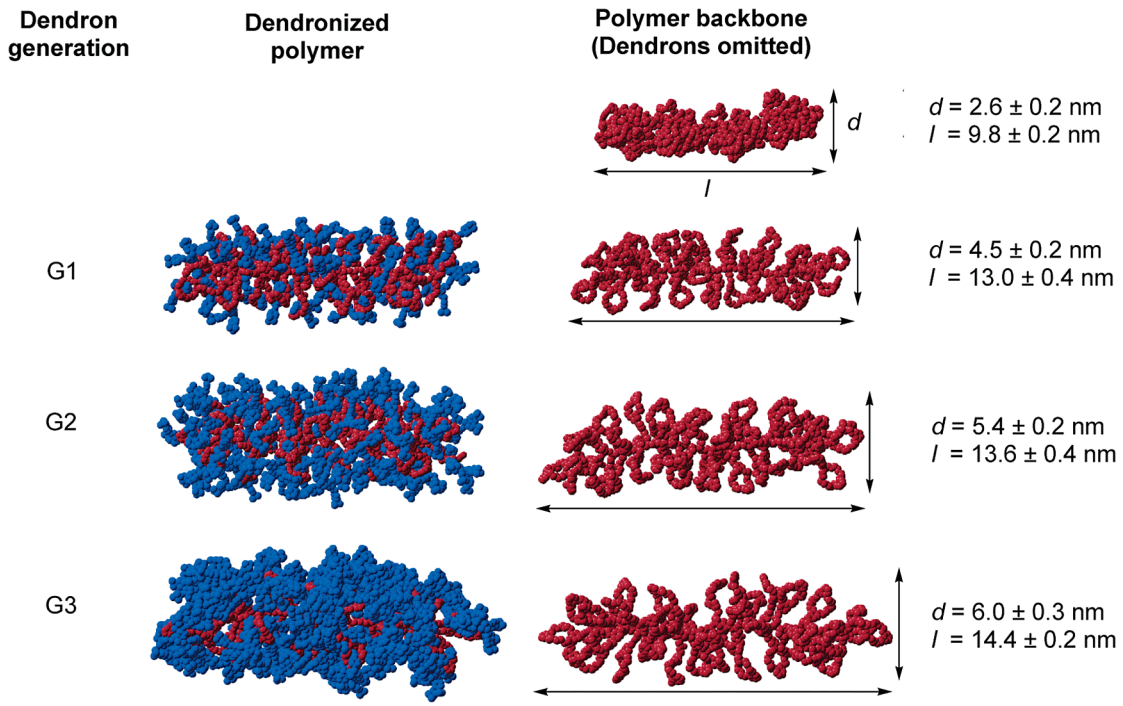

Figure 9. Molecular dynamics simulations (AMBER*, $CHCl_3$, 300 ps) of the [G1]−[G3]-DPAs [**1a**−**c**-H·PF_6]$_n$⊂**2** and their polymer backbones (red) with omitted dendrons (blue) (d = diameter and l = length).

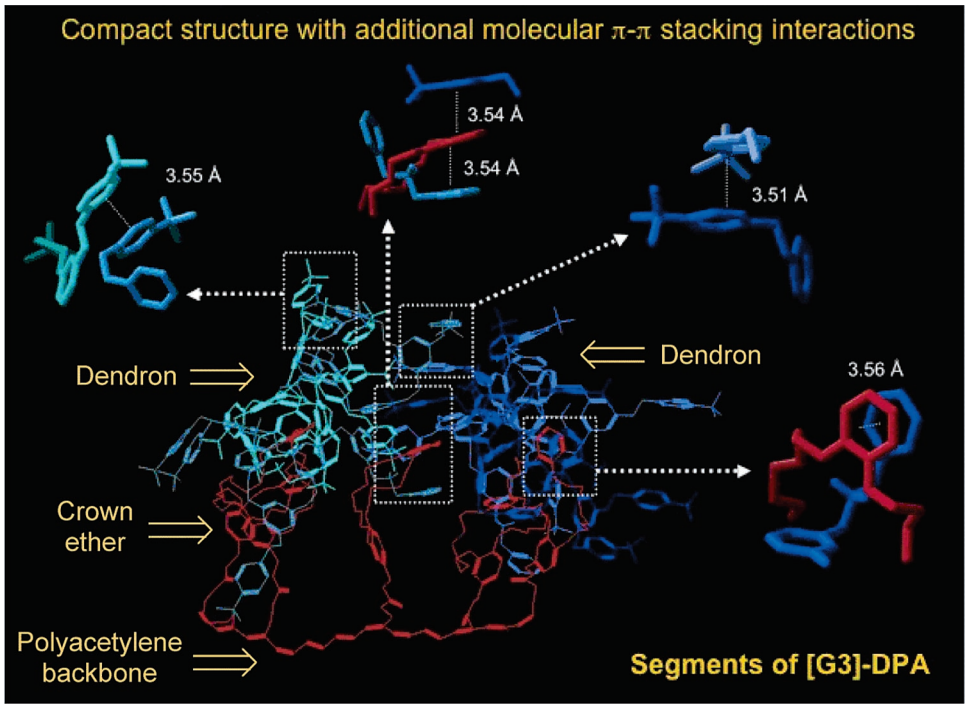

Figure 10. Molecular dynamics simulations showing a segment of [G3]-DPA [**1c**-H·PF_6]$_n$⊂**2** with $\pi-\pi$ stacking interactions in its closely packed superstructure.

the increasing generation of the DPAs. It reveals that the extension of the polyacetylene backbone after the attachment of dendrons is the origin for the red-shifting observation in their UV/visible absorptions. Furthermore, the simulations also revealed (Figure 10) that the DPAs exhibit additional $\pi-\pi$ stacking interactions (~3.5 Å) between the multiple aryl units in their closely packed superstructures, most notably in the case of the [G3]-dendrons. These additional interactions are crucial for the stabilization of the self-assembled, supramolecular dendronized polymers.

(16) Although the AFM imaging conditions used are considered to yield topographical information closest to the actual height, flattening of the molecules caused by compression and height artifacts resulting from adhesive interactions can be responsible for the lower height measured in our studies.
(17) Weiner, S. J.; Kollman, P. A.; Case, D. A.; Singh, V. C.; Ghio, C.; Alagona, G.; Profeta, S.; Weinre, P., Jr. *J. Am. Chem. Soc.* **1986**, *106*, 765−784.
(18) Still, W. C.; Tempczyk, A.; Hawler, R. C.; Hendrickson, T. *J. Am. Chem. Soc.* **1990**, *112*, 6127−6129.
(19) Mohamadi, F.; Richards, N. G. J.; Guida, W. C.; Liskamp, R.; Lipton, M.; Caufield, C.; Chang, G.; Hendrickson, T.; Still, W. C. *J. Comput. Chem.* **1990**, *11*, 440−467.

Conclusion

The successful preparation of the acid−base switchable [G1]- to [G3]-supramolecular dendronized polymers has been demonstrated by simply mixing suitable amounts of dendritic ammonium salts with side-chain functionalized crown-ether polymers. Conformational changes in the polymer backbone are induced by the attachment of dendrons, which were characterized by GPC, LS, and UV/visible spectroscopy. Both the experimental and simulation results are consistent, which confirmed that, as the size of the attached dendron increases, the length of extension of the polymer backbone also increases. Furthermore, reversible acid−base switching of the dendronized polymers can be performed in solution. The polymers exhibited a good stability even after several cycles of the acid−base switching processes. By taking advantage of the synthetic control of (a) the degree of polymerization, (b) the distance between each molecular recognition unit, and (c) the sizes of the dendron, new opportunities exist to control the stiffening of conformations of the polymer, allowing for the development and fabrication of nano-architectures.

Experimental Section

Materials. Pyridinium chlorochromate (PCC, 98%), benzylamine (redistilled, ≥99.5%), hydrogen hexafluorophosphate (60 wt. % in H_2O), 4-pentynoic acid (95%), *N*,*N*'-dicyclohexylcarbodiimide (DCC, 99%), 4-(dimethylamino)pyridine (DMAP, 99%), sodium hydride (dry, 95%), sodium borohydride (99%), triethylamine (99.5%), methanol (anhydrous, 99.8%), tetrahydrofuran (THF, anhydrous, 99.9%, inhibitor free), and poly(vinylbenzyl chloride) (60/40 mixture of 3- and 4-isomers with $M_w \approx 100$ kDa and $M_n \approx 55$ kDa) were purchased from Aldrich. Chloro(norbonadiene)rhodium(I) dimer ($[Rh(nbd)Cl]_2$, nbd = norbonadiene) was purchased from Acros Organics. Dichloromethane (HR-GC grade, 99.9%), ethyl acetate (99.9%), hexane (99.8% minimum, 85% as *n*-hexane), and toluene (99.9%) were purchased from EMD. All purchased chemicals are used without further purification. Dendritic alcohols **4a**,[13] **4b**,[13] dendritic ester [G3]-CO_2Me,[13] and DB24C8-alcohol **6**[14] were prepared (all of purity ≥98%) according to literature procedures. Compounds **1a**−**c**-H·PF_6, **5a**−**c**, and **7** were synthesized and isolated with purities in excess of 98%.

Techniques. All reactions were carried out under an argon atmosphere. Thin-layer chromatography (TLC) was performed on silica gel sheet 60F_{254} (Merck). Column chromatography was performed on silica gel 60F (Merck 9385, 0.040−0.063 mm). All nuclear magnetic resonance (NMR) spectra were recorded on a Bruker Avance 500 (^{1}H: 500 MHz; ^{13}C: 126 MHz), and $CDCl_3$ was used as a solvent unless otherwise stated. Chemical shifts are reported as parts per million (ppm) downfield from signal of Me_4Si as internal standard for ^{1}H and ^{13}C NMR spectroscopy. High-resolution electrospray ionization (HR-ESI) mass spectra were measured on an IonSpec Fourier transform mass spectrometer. High-resolution matrix-assisted laser desorption/ionization spectra (HR-MALDI) were measured either on an IonSpec Fourier transform mass spectrometer or an AppliedBiosystems DE-STR MALDI time-of-flight mass spectrometer. The reported molecular mass (*m*/*z*) values were the most abundant monoisotopic mass. UV/visible spectra were recorded on a Varian Cary 100 Bio UV−visible spectrophotometer. Melting points were determined on an Electrothermal 9100 digital melting point apparatus and are uncorrected.

A. General Synthetic Procedure for [G1]−[G3] Dendritic Aldehydes 5a−c. A mixture of the appropriate dendritic alcohol **4a**−**c** and PCC (1.5 equiv) in CH_2Cl_2 was stirred at 25 °C for 2 h. The reaction mixture was then filtered through a short pad of Celite, and the collected filtrate was concentrated under reduced pressure. The residue was then purified by column chromatography (SiO_2) using hexane/EtOAc as an eluent to afford the products **5a**−**c**.

5a. Following the general synthetic procedure A, a mixture of the [G1]-dendritic alcohol **4a**[13] (4.1 g, 9.5 mmol), PCC (3.1 g, 14 mmol) in CH_2Cl_2 (50 mL) was stirred for 2 h. Purification using column chromatography (hexane/EtOAc = 5:1 gradient to 3:1) afforded the aldehyde **5a** (3.6 g, 88%) as a white solid. Mp = 96.2−99.6 °C; ^{1}H NMR: 1.34 (s, 18 H), 5.05 (s, 4 H), 6.88 (t, J = 2.3 Hz, 1 H), 7.12 (d, J = 2.3 Hz, 2 H), 7.37 (d, 8.3 Hz, 4 H), 7.43 (d, 8.3 Hz, 4 H), 9.91 (s, 1 H); ^{13}C NMR: 31.2, 34.5, 70.2, 108.1, 108.5, 125.5, 127.5, 133.1, 138.3, 151.2, 160.4, 191.8; MS(HR-ESI): calcd for $C_{29}H_{34}O_3$ *m*/*z* = 430.2508; found *m*/*z* = 430.2513 [M^+, 100%].

5b. Following the general synthetic procedure A, a mixture of the [G2]-dendritic alcohol **4b**[13] (0.30 g, 0.31 mmol), PCC (0.10 g, 0.46 mmol) in CH_2Cl_2 (10 mL) was stirred for 2 h. Purification using column chromatography (hexane/EtOAc = 4:1) afforded the aldehyde **5b** (270 mg, 90%) as a white solid. Mp = 101.6−105.2 °C; ^{1}H NMR: 1.33 (s, 36 H), 5.00 (s, 8 H), 5.03 (s, 4 H), 6.60 (t, J = 2.3 Hz, 2 H), 6.68 (d, J = 2.3 Hz, 4 H), 6.86 (t, J = 2.3 Hz, 1 H), 7.09 (d, J = 2.3 Hz, 2 H), 7.36 (d, 8.3 Hz, 8 H), 7.39 (d, 8.3 Hz, 8 H), 9.89 (s, 1 H); ^{13}C NMR: 31.2, 34.5, 69.9, 70.2, 101.5, 106.2, 108.2, 108.6, 125.46, 125.54, 127.5, 133.5, 138.3, 151.0, 160.20, 160.22, 191.8; MS(HR-MALDI): calcd for $C_{65}H_{74}O_7Na$ *m*/*z* = 989.5332; found *m*/*z* = 989.5362 [$(M + Na)^+$, 100%].

5c. A solution of [G3]-CO_2Me[13] (0.32 g, 0.16 mmol) in THF (3 mL) was added to a slurry of $LiAlH_4$ (12 mg, 0.31 mmol) in THF (3 mL) at 0 °C. The mixture was stirred for 2 h and then quenched by water, extracted with EtOAc twice (20 mL), washed with brine, dried ($MgSO_4$), and filtered. The filtrate obtained was evaporated under reduced pressure to afford a colorless glassy solid. Subsequently, following the general synthetic procedure A, a mixture of the colorless glassy solid and PCC (67 mg, 0.31 mmol) in CH_2Cl_2 (5 mL) was stirred for 2 h. Purification using column chromatography (hexane/EtOAc = 4:1) afforded the aldehyde **5c** (0.31 g, 94%) as a colorless glassy solid. ^{1}H NMR 1.30 (s, 72 H), 5.03 (s, 24 H), 5.32 (s, 4 H), 6.52 (t, J = 2.3 Hz, 4 H), 6.56 (d, J = 2.3 Hz, 2 H), 6.65−6.67 (m, 12 H), 6.83 (t, J = 2.3 Hz, 1 H), 7.07 (d, J = 2.3 Hz, 2 H), 7.34 (d, 8.3 Hz, 16 H), 7.38 (d, 8.3 Hz, 16 H), 9.83 (s, 1 H); ^{13}C NMR: 31.1, 34.4, 69.8, 70.0, 101.4, 106.1, 108.1, 108.5, 125.5, 127.4, 133.4, 138.2, 151.0, 160.20, 160.21, 191.7; MS(HR-MALDI): calcd for $C_{137}H_{154}O_{15}Na$ *m*/*z* = 2062.1185; found *m*/*z* = 2062.1408 [$(M + Na)^+$, 100%].

B. General Synthetic Procedure for [G1]−[G3] Dendritic Dialkylammonium Salts 1a−c-H·PF$_6$. A mixture of the dendritic aldehydes **5a**−**c** and benzylamine (1.1 equiv) in PhMe equipped with a Dean−Stark apparatus was heated under reflux for 2 h. The excess of solvent was then removed under reduced pressure, and the remaining solid was redissolved into anhydrous MeOH/THF (1:1 v/v). Subsequently, $NaBH_4$ (3 equiv) was added to the mixture at 0 °C. The reaction mixture was then stirred at 25 °C for 6 h. H_2O was added dropwise to quench the reaction, and the resulting mixture was extracted with EtOAc twice. The combined organic layers were dried ($MgSO_4$) and filtered, and the filtrate was evaporated under reduced pressure to afford a white solid. Subsequently, the residue was redissolved into THF, and a solution of HPF_6 (2 equiv) was added dropwise at 0 °C and stirred for 30 min. Then, H_2O was carefully added to quench the reaction, and the resulting mixture was extracted with CH_2Cl_2 twice. The combined organic layers were dried (Na_2SO_4) and filtered, and the filtrate was evaporated under reduced pressure to afford the products **1a**−**c**-H·PF_6.

1a-H·PF$_6$. Following the general synthetic procedure B, starting from the aldehyde **5a** (3.0 g, 7.0 mmol), benzylamine (0.84 mL, 7.7 mmol), and $NaBH_4$ (0.80 g, 21 mmol), the ammonium salt **1a**-H·PF_6 (2.5 g, 73%) was obtained as a white solid. Mp = 138.4−144.8 °C; ^{1}H NMR (CD_2Cl_2): 1.27 (s, 18 H), 3.91 (bs, 2 H), 3.96 (bs, 2 H), 4.96 (s, 4 H), 6.59 (t, J = 2.3 Hz, 1 H), 6.62 (d, J = 2.3 Hz, 2 H), 7.28−7.42 (m, 13 H), 8.40 (bs, 2 H); ^{13}C NMR (CD_3CN): 30.4, 34.1, 51.0, 51.1, 69.6, 102.7, 108.8, 125.4, 127.6, 128.9, 129.6, 130.1, 130.3, 132.5, 133.7, 151.1, 160.2; MS(HR-ESI): calcd for $C_{36}H_{44}NO_2$ *m*/*z* = 522.3367; found *m*/*z* = 522.3362 [$(M - PF_6)^+$, 100%].

1b-H·PF$_6$. Following the general synthetic procedure B, starting from the aldehyde **5b** (0.30 g, 0.31 mmol), benzylamine (0.037 mL, 0.34 mmol), and $NaBH_4$ (36 mg, 0.93 mmol), the dendritic dialkylammonium salt **1b**-H·PF_6 (0.28 g, 74%) was obtained as a colorless glassy solid. ^{1}H NMR (CD_2Cl_2): 1.29 (s, 36 H), 3.82 (bs, 2 H), 3.88 (bs, 2 H), 4.90−4.97 (m, 12 H), 6.51 (d, J = 2.3 Hz, 2 H), 6.57 (t, J = 2.3 Hz, 1 H), 6.65 (d, J = 2.3 Hz, 4 H), 6.74 (t, J = 2.3 Hz, 2 H), 7.25−7.42 (m, 21 H), 9.28 (bs, 2 H); ^{13}C NMR (CD_3CN) 29.9, 30.9, 34.3, 49.4, 69.7, 69.9, 101.2, 106.2, 108.7, 125.3, 127.4, 129.0, 129.4, 129.8, 130.0, 133.7, 138.9, 151.0, 160.07, 160.12; MS(HR-ESI): calcd for $C_{72}H_{84}NO_6$ m/z = 1058.6293; found m/z = 1058.6341 [(M − PF_6)$^+$, 100%].

1c-H·PF$_6$. Following the general synthetic procedure B, starting from the aldehyde **5c** (0.30 g, 0.15 mmol), benzylamine (0.018 mL, 0.17 mmol), and $NaBH_4$ (17 mg, 0.45 mmol), the dendritic dialkylammonium salt **1c**-H·PF_6 (0.24 g, 70%) was obtained as a colorless glassy solid. ^{1}H NMR (CD_2Cl_2): 1.29 (s, 72 H), 3.82 (bs, 2 H), 3.88 (bs, 2 H), 4.92−4.99 (m, 28 H), 6.50−6.54 (m, 7 H), 6.64−6.67 (m, 14 H), 7.27−7.44 (m, 37 H), 8.40 (bs, 2 H); ^{13}C NMR (CD_3CN) 29.7, 30.8, 34.2, 49.3, 69.6, 69.8, 101.2, 106.21, 106.22, 108.6, 125.2, 127.3, 128.9, 129.3, 129.7, 130.0, 133.6, 138.8, 150.9, 160.0, 160.1; MS(HR-ESI): calcd for $C_{144}H_{164}NO_{14}$ m/z = 2131.2146; found m/z = 2131.1965 [(M − PF_6)$^+$, 100%].

Monomer 7. A mixture of the DB24C8-alcohol **6**[14] (0.17 g, 0.36 mmol), 4-pentynoic acid (40 mg, 0.40 mmol), DCC (0.15 g, 0.71 mmol), and DMAP (9.0 mg) in CH_2Cl_2 (3 mL) was stirred at 25 °C for 12 h. The solution was then filtered through a short pad of Celite, and the filtrate obtained was evaporated under reduced pressure. The residue was purified by column chromatography (EtOAc) to afford the monomer **7** (0.13 g, 66% yield) as a white solid. Mp = 91.2−94.8 °C; ^{1}H NMR: 1.97 (s, 1 H), 2.46 (m, 2 H), 2.56 (m, 2 H), 3.83 (s, 8 H), 3.91 (q, J = 2.1 Hz, 8 H), 4.15 (quin, J = 2.1 Hz, 8 H), 5.04 (s, 2 H), 6.80−6.92 (m, 7 H); ^{13}C NMR: 14.2, 33.3, 66.4, 69.0, 69.25, 69.30, 69.4, 69.7, 69.8, 71.2, 82.3, 113.4, 113.9, 114.2, 121.3, 121.7, 128.6, 148.7, 148.8, 148.9, 171.5; MS(HR-MALDI): calcd for $C_{30}H_{38}O_{10}Na$ m/z = 581.2363; found m/z = 581.2371 [(M + Na)$^+$, 100%].

PA-DB24C8 2. A degassed mixture of the monomer **7** (0.13 g, 0.23 mmol), $[Rh(nbd)Cl]_2$ (11 mg, 0.023 mmol) and Et_3N (0.032 mL, 0.23 mmol) in CH_2Cl_2 (1 mL) was stirred at 25 °C for 24 h. The excess of solvent was evaporated under reduced pressure, and the residue was redissolved into a minimum amount of CH_2Cl_2. Subsequently, the CH_2Cl_2 solution was precipitated onto cold hexanes/CH_2Cl_2 (100:1, 400 mL), and the precipitate was redissolved in CH_2Cl_2 and then evaporated under reduced pressure to give the polyacetylene PA-DB24C8 **2** (0.12 g, 90% yield) as a brown amorphous solid. ^{1}H NMR (CD_2Cl_2): 2.30−2.70 (br, 4 H), 3.65−3.75 (br, 8 H), 3.79−3.85 (br, 8 H), 4.05−4.15 (br, 8 H), 4.86 (brs, 1 H), 5.00 (brs, 2 H), 6.80−6.92 (br, 7 H); ^{13}C NMR (CD_2Cl_2): 24.9, 33.8, 65.9, 69.20, 69.25, 69.6, 69.7, 70.87, 70.89, 113.9, 114.4, 114.5, 121.3, 121.4, 126.3 (C═C), 129.2 (C═C), 148.9, 149.00, 149.04, 172.4; LS: M_w = 18 kDa, M_n = 13 kDa, and PDI = 1.4; GPC: M_w = 15 kDa, M_n = 9.3 kDa, and PDI = 1.6.

PS-DB24C8 3. NaH (56 mg, 2.3 mmol) was added portionwise to a solution of the DB24C8-alcohol **6** (0.91 g, 1.9 mmol) in degassed THF/CH_2Cl_2 (1:1, 10 mL) at 0 °C. The mixture was stirred for 30 min at 0 °C. Subsequently, a solution of poly(vinylbenzyl chloride) (0.50 g, 1.6 mmol) in degassed THF/CH_2Cl_2 (1:1, 10 mL) was added dropwise to the reaction mixture. After 24 h, H_2O was added to quench the reaction, and the resulting mixture was extracted with CH_2Cl_2 twice (2 × 20 mL). The combined organic layers were dried ($MgSO_4$) and filtered, and the filtrate was evaporated under reduced pressure. The residue was then precipitated onto cold hexanes/CH_2Cl_2 (50:1, 800 mL) to afford the polystyrene PS-DB24C8 **3** (0.82 g, 93% yield, ∼50% crown ether attachment determined by LS and ^{1}H NMR spectroscopy) as a white solid. ^{1}H NMR ($CDCl_3$): 1.25−1.50 (br, 4 H), 1.50−1.80 (br, 2 H), 3.83 (brs, 8 H), 3.91 (brs, 8 H), 4.15 (brs, 8 H), 4.23−4.45 (br, 4 H), 4.54 (s, 2 H), 6.20−6.55 (br, 4 H), 6.75−7.16 (m, 11 H); LS: M_w = 140 kDa, M_n = 85 kDa and PDI = 1.7.

Molecular Dynamics Simulations. Molecular dynamics simulations were performed using the program Maestro v3.0.038 package (Schrödinger, Inc., Portland, OR). The AMBER* force field and GB/SA solvent model for $CHCl_3$ were used along with an extended cutoff for nonbonded interactions. The SHAKE algorithm was employed on all bonds to hydrogens throughout the simulations. Structures for PA-DB24C8 **2** and [G1]−[G3]-DPAs [**1a**−**c**-H·PF_6]$_n$⊂**2** were constructed with a degree of polymerization of 40. No counterions were present in the simulations of [G1]−[G3]-DPAs [**1a**−**c**-H·PF_6]$_n$⊂**2**. A 300 ps molecular dynamics simulation (1.5 fs time step) at an elevated temperature of 400 K was used to equilibrate each structure. A simulation of 300 ps was sufficiently long to ensure that the standard energetic deviation was less than 0.01% of the total energy for each polymer, implying full equilibration. Structures generated from each molecular dynamics simulation were then energy minimized to full convergence at 298 K using the PRCG algorithm.

Laser Light Scattering. Dynamic light scattering (LS) was performed to determine the hydrodynamic radii of the polymers by using a Brookhaven Instruments at an angle of 90° using a He−Ne laser (632.8 nm), and CONTIN program was used for curve fitting. Dynamic LS was also employed to measure the molecular weights by using a Beckman Coulter N4 Plus PCS submicrometer particle size analyzer with a 90° detector angle (He−Ne laser, 632.8 nm) using the molecular weight mode after sonication of the samples. All samples were dissolved in CH_2Cl_2 and filtered with a membrane filter (Whatman PTFE GD/X) with a nominal pore size of 0.45 μm before making measurements at 293 K.

Gel Permeation Chromatography. Gel permeation chromatography (GPC) was performed from a setup of a Varian Dynamax SD-200 solvent delivery system, equipped with a Waters Ultrastyragel HR3 (7.8 mm × 300 mm) column and a Dynamax PDA-2 photodiode array detector. CH_2Cl_2 (flow rate = 1.0 mL/min, column temperature = 25 °C) was used as the eluent, and the system was calibrated using polystyrene standards (Aldrich). All samples were sonicated and filtered through a membrane filter (Whatman PTFE GD/X, 0.45 μm) before the measurements.

Atomic Force Microscopy. Atomic force microscopy (AFM) was performed by using a multimode Nanoscope IIIA system (Digital Instruments, Santa Barbara, CA) operated in tapping mode using silicon cantilevers having either a nominal spring constant of 0.3 N/m (resonance frequency = 21 kHz) or 0.9 N/m (resonance frequency = 60 kHz). AFM images were acquired as 512 pixels × 512 pixels with a scan rate of 1.00 Hz.

Acknowledgment. We thank the MARCO and its focus center FENA for financial support and Croucher Foundation (HKSAR) for a fellowship to K.C.-F.L. We acknowledge discussions with E.J. Kramer (UCSB) as well as the use of the MRL Central Facilities supported by the MRSEC Program (DMR05-20415) of the National Science Foundation.

Supporting Information Available: Proton NMR spectra of the dendronized polymers in addition to complete refs 1, 4e, 5b, 6b, 10c, 11a, and 13. This material is available free of charge via the Internet at http://pubs.acs.org.

JA058151V